Diffractive optics for precision alignment in the framework of the EUCLID space telescope mission

Jean-Michel Asfour[a], Christof Bodendorf[b], Andreas Bode[b], Frank Grupp[b], Ralf Bender[b], Frank Weidner[a], A.G. Poleshchuk[c], R.K. Nasyrov[c]
[a]Dioptic GmbH, Bergstreet, 69469 Weinheim, Germany,
[b]Max Planck Institute for Extraterrestrial Physics, Gießenbachstreet, 85748 Garching, Germany,
[c]Institute of Automation and Electrometry SB RAS, Novosibirsk, 630090, Russia

ABSTRACT

We present a procedure to precisely align lens elements using specific diffractive optics with an integrated transmission flat (Diffractive Fizeau Null Lens, DFNL) which serves as reference surface for a Fizeau interferometer. The method is used for aligning the optical assembly of the near-infrared spectrometer and photometer of the Euclid space telescope, which is currently being developed in the framework of the ESA Cosmic Vision 2015 - 2025 Program [1,2]. Each lens has a corresponding annular zone on a multi-zonal computer-generated hologram to control its position. The alignment sensitivity is well below 1 µm. The achieved alignment accuracy of the lenses relative to each other depends mainly on the long-time stability of the integration tower. Error budgets of the utilized computer-generated holograms and physical limitations are analyzed. Calibration measurements and the typically reached alignment accuracies are shown and discussed.

Keywords: diffractive optics, computer generated holograms, lens alignment, precision optics, telescope, interferometry, space optics

1. INTRODUCTION

In the field of precision metrology for aspheric surfaces, the use of *Computer-Generated Holograms* (CGHs) is quite common. Using CGHs, one can transform spherical into aspherical wave fronts, which resemble the nominal shape of an aspherical surface under test. The corresponding rays are thus normal to the surface, and reflected backwards into themselves. This is the autocollimation condition, used for interferometrical methods, which are thus available also for asphere metrology. In doing so, one is typically interested in detecting surface irregularities. Interferometrical measurement results can be analyzed using the Zernike polynomials, which are an orthogonal basis system over a circular disk. For optical manufacturing, the first Zernike coefficients, representing piston, tilt and defocus, are usually of no interest. Tilt and power contributions can be cancelled by appropriately aligning the interferometric measurement setup and the remaining portions are normally regarded as adjustment artifacts, which are numerically subtracted, using the 'remove tilt' and 'remove power' click boxes of the evaluation software.

In this paper, we want to point out, that these simple mouse clicks remove powerful and extremely sensitive alignment signals. Using them successively to several optical elements in a row, leads to a highly accurate alignment procedure along a straight axis, defined by an appropriate multi-zonal CGH. This concept is used for aligning a four-lens optical assembly of the EUCLID space telescope [1,2,3,4,5]. The EUCLID optics has very high demands on alignment accuracy and stability. In this paper, we explain the concept of using a Fresnel zone plate CGH with multiple zones for aligning purposes, its manufacturing accuracies and the corresponding limits concerning the generated wavefronts. A comparison of the theoretical performance with experimental investigations will be shown to yield promising results, which satisfy the requirements well.

2. NISP OPTICAL ASSEMBLY AND ALIGNMENT PROCEDURE

The European Space Agency (ESA) is currently developing the space telescope 'Euclid', which addresses fundamental cosmological questions related to the large-scale distribution of dark matter and the essence of dark energy [1,2]. The mission will be equipped with an f/20 Korsch type telescope using a 1.2 m primary mirror. It has a visual channel and a near infrared spectrographic and photometric (NISP) channel [3,4]. The NISP optical assembly [5,6] consists of a

spherical-aspherical meniscus type corrector lens (CL), a filter- and a grism wheel and three spherical-aspherical meniscus type lenses L1, L2 and L3 (Figure 1). The lens elements need to be aligned against each other with very tight mechanical tolerances in the micrometer range. The adjustment hast to be done according to the warm positions, while the final positions are reached not until the operating temperatures of 133 K in space[4]. The lens positions have to be stable throughout the launch [6].

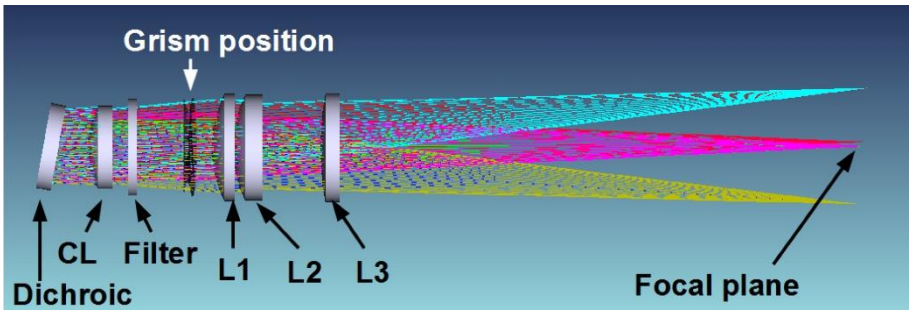

Figure 1. Optical assembly of Euclid's near infrared spectrometer and photometer.

CGHs for asphere tests generate wavefronts with continuously changing radius of curvature as a function of the radial distance from the centre to the outer margin. They are designed to resemble the nominal aspherical surface under test. *Multi-Zone-CGHs* (MZ-CGHs) follow a similar approach. However, the important difference is that the radius of curvature of the generated wavefront experiences discontinuous jumps at the zone edges. The wavefront therefore separates into a series of annular subareas (Figure 2). In the presented case, all subareas build spherical wavefronts, each with a different focal length. Accordingly, a series of spots along a straight line arises. The thus defined *optical axis* serves as *reference* for the interferometric adjustment procedure of the lenses. The straightness of this axis is the key feature of the presented method.

The lens alignment is performed according to the following procedure: The MZ-CGH is mounted on the bayonet lock of a Fizeau interferometer (Figure 2b). Next, the green plane wave (Figure 2a) is interferometrically aligned normal to a plane reference surface. In the simple case, which we present here, the mechanical setup (which is beyond the scope of the current paper) ensures, that the lenses are not tilted relative to the reference surfaces.

Now, the lenses are inserted in the sequence L3, L2, L1. The spherical surface of each lens is sampled with the corresponding annular wavefront subarea, which defines accurately its nominal position. A lens positioning error along the optical axis is detected as Zernike *defocus* term in the wavefront. A centering error in the lateral plane is observed as a Zernike *tip/tilt* term. The correct position is reached, if the fringes of the interference pattern are perfectly nulled. In this case, the centres of curvature of the lenses coincide with the corresponding spot positions.

The layout according to Figure 2a shows two more zones. They provide signals from the *cat-eye* positions at the vertices of L3 and L1. As they have a larger numerical aperture (NA) than the zones that sample the surfaces (autocollimation position), the Zernike defocus term is *more sensitive* to the distance in z [7]. And unlike the autocollimation positions, the cat-eyes are independent of the actual radius of curvature of the lenses. Furthermore, the cat-eye zone belonging to L3 has a *rectangular* shape and crosses all annular zones (Figure 2b). The large radial range of this zone is optimized for defocus measurements. It improves the initial z-positioning of the interferometer. Cat-eye positions carry however no centering information of the lenses.

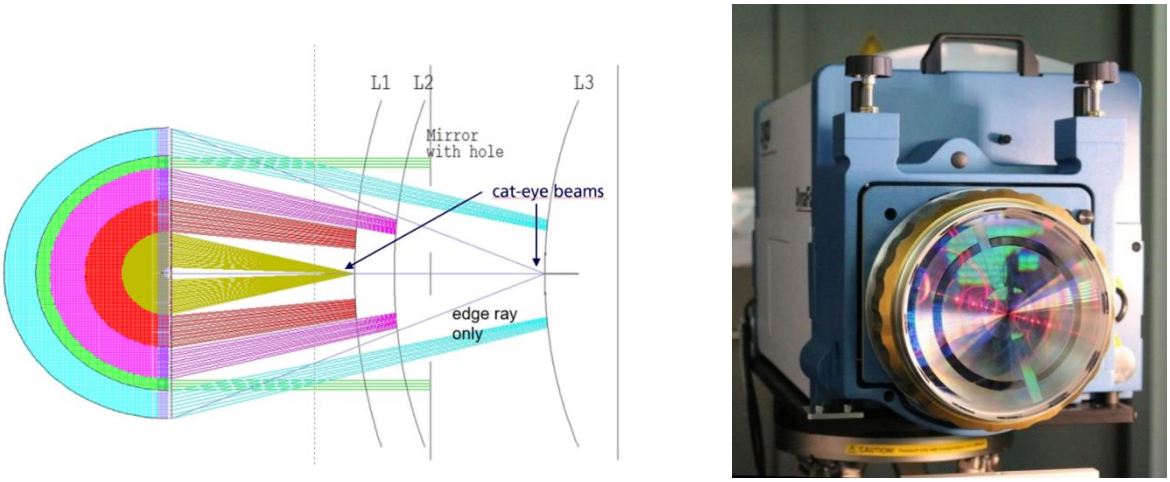

a b

Figure 2. CGH design with six different FZP zones (a).
Photograph of the MZ-CGH, mounted on the bayonet lock of a Fizeau interferometer (b).

3. MANUFACTURING OF THE MZ-CGH

For manufacturing CGHs, a specifically designed laser-lithographic high precision polar coordinate circular laser writing system (CLWS) has been designed and built at the IA&E SB RAS [8,9,14,15]. This system can produce very precise rotationally symmetric and also arbitrary shaped diffractive structures in a chromium layer on optical substrates. The lithographic process does not need any photoresist, it works with a high-power laser, which directly exposes a chromium layer.

Figure 3 shows a schematic layout of the CLWS. The optical substrate with the chromium based recording layer is fixed on a 300 mm faceplate, which is part of an air-bearing spindle. An angular encoder and frequency multiplier form clock pulses ($\sim 4 \cdot 10^6$ per revolution) which are used to synchronize the laser writing beam modulation with the substrate rotation. A linear air bearing translation stage and the linear drive move the optical writing head across the radial coordinate. A laser interferometer serves for the precise position control of the writing head, having a positioning resolution of approx. 0.6 nm. The absolute accuracy of the laser beam positioning is approx. 10 nm. The CLWS is equipped with two different solid-state lasers with 405 nm and 532 nm wavelength respectively [10,11].The first laser is used for photoresist lithography and the second laser with 2W of power is used for writing directly into chromium films. Two acousto-optic modulators (AOM 1 and AOM 2) control the beam power of the both lasers with high dynamic range. The writing head is equipped with a laser based autofocus system, a microscope head with CCD camera, photodetectors and deflector and forms a writing spot with a spot diameter of < 0.5 μm FWHM. Using higher intensities of the laser, the line width can be enlarged up to 1.5 μm. Detailed specification of the CLWS can be found in table 1.

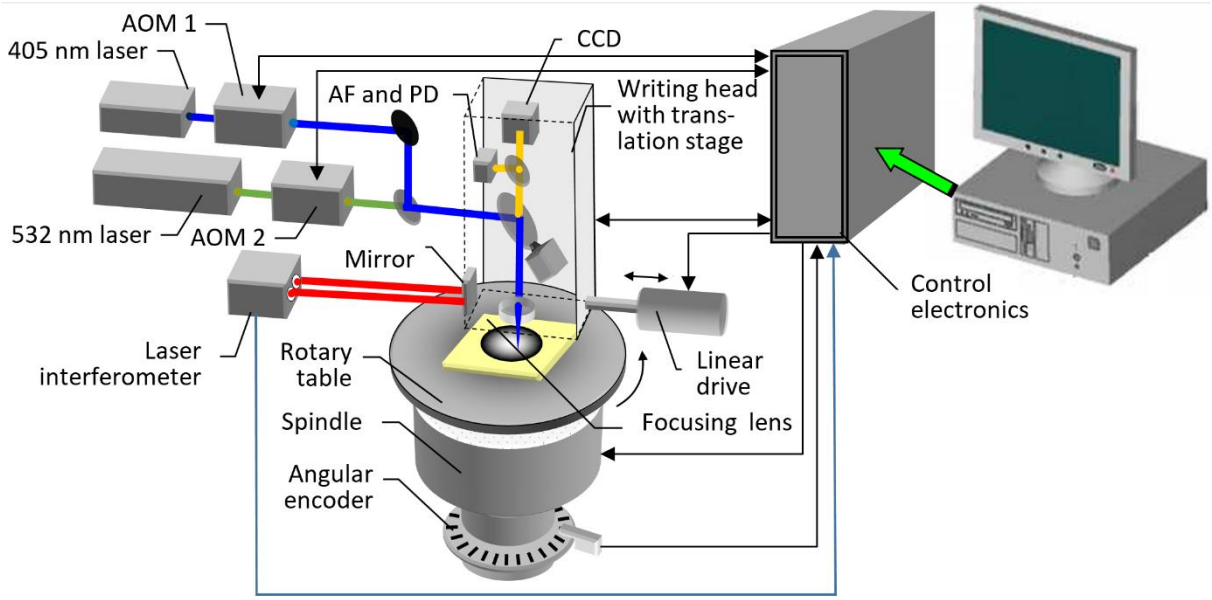

Figure 3. Schematic layout of the circular laser writing system (CLWS).

Table 1. Performance and Specifications of the laser writing systems.

Parameter Name	Value
Maximum diameter of the writing field	300 mm
Substrate thickness	1.5–24 mm
Recording spot diameter	0.5 μm
Rotation speed	300–800 rpm
Accuracy of radial coordinate positioning (rms)	0.02 μm
Accuracy of angular coordinate measurement (rms)	~1 arc sec
Recording wavelength	457–514-nm, Ar laser
Writing time with ~0.5-μm pitch on a 90-mm diameter field	2 h
CLWS dimensions / weight	1.5 x 1 x 1.4 m^3/1.2t

Direct Laser Writing process

The CLWS allows the fabrication of CGHs with binary or continuous-relief microstructures onto mechanically stable, thick and large optical substrates. The CGH pattern can be created either by using a photoresist based lithography or by a so called laser direct writing method, which is based on a thermochemical effect of a laser induced local heating of the chromium film [12]. This process is used for creating binary CGHs and is shown in Figure 4a. The laser induced heating of the chromium film creates a thin oxide layer (stage I in Figure 4a). After exposure, the substrate is immersed in a caustic bath to develop the written pattern (stage III). The bare chromium is dissolved faster than the chromium with oxide layer on top. The chromium pattern on the substrate can be used as amplitude CGH (stage III). The chromium film can be easily deposited also on curved surface. It allows a lithographic process on weak concave or convex surfaces. Using a subsequent reactive ion beam etching, the amplitude CGH can be transformed into a phase binary CGH (stage IV). In this case, the chromium pattern is used as a protective mask, while the ion beam is etching into the bare substrate. In the last stage (stage

V), the residual chromium is removed again by wet chemical etching and the phase CGH is ready for use. This thermochemical lithography process has a spatial resolution of 1500 -2000 mm^{-1} (Figure 4 b,c), with subsequent phase etching it is slightly smaller (600-800mm^{-1}).

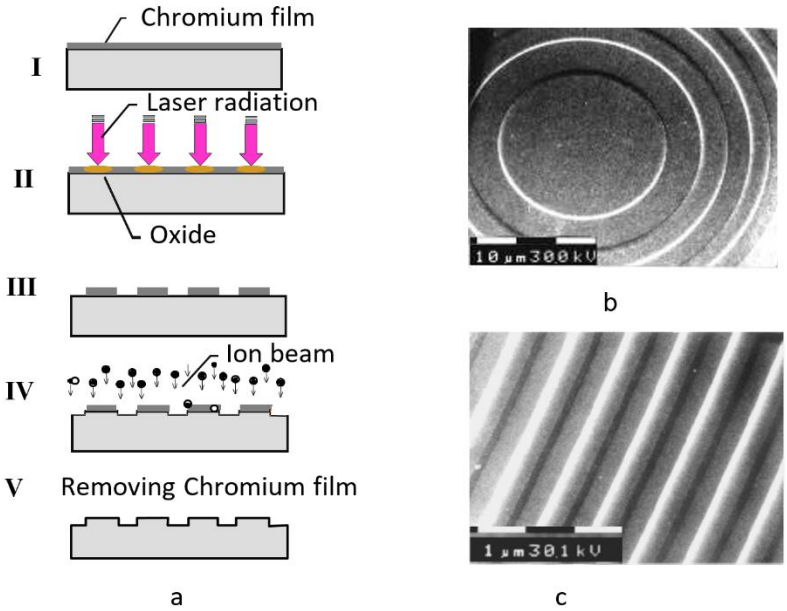

Figure 4. Lithographic process for creating binary CGHs (a),
typical examples of diffractive patterns in the center (b) and in the periphery (c).

Fabrication errors

The lithographic writing process has several limitations concerning the accuracy of the generation of the CGH structures [13,14]. These manufacturing errors have two components: the difference between the calculated and the real coordinates of the CGH pattern, and the difference between the ideally symmetric binary amplitude or phase profile and the realized profile.

The absolute error of the structured coordinates depends on the accuracy of the position of the writing head with respect to the substrate. Coordinate error results in an additional phase shift of the wavefront of the light flux transmitted through the fabricated CGH. The phase shift is similar to the phase shift caused by disturbance of the periodicity of grooves in a usual diffractive grating and leading to the appearance of parasitic diffraction orders. The phase shift (in fractions of light wavelength λ) can be defined as [13]:

$$\Delta W(x,y) = - m \lambda \varepsilon(x,y) / S(x,y),$$

where m is the diffraction order, S(x,y) is the nominal local grating spacing, $\varepsilon(x,y)$ is the positioning error of the local grating spacing perpendicular to the grating lines, or more precisely $\varepsilon_i = r_i' - r_i$, where r_i and r_i' are the nominal and the real positions of the grating line 'i'. From this equation one can see, that the knowledge of the local grating line position error ε across the whole aperture allows the analysis of the wavefront error related to the positioning error. In the case of a rotationally symmetric CGH created by the CLWS, the problem of measuring ε becomes a one-dimensional task.

A list of different effects which introduce writing errors and the taken measurements for reducing them are given in Table 2. These various actions for increasing the patterning accuracy lead to a final radial positioning accuracy of 3.5 nm rms [15,16,17,18,19].

Table 2. Different sources of CLWS patterning error and methods for reducing them

Error type	Methods for error reduction
Zeroing error of the origin of coordinates	Accurate search of rotation axis
Drift of the origin of coordinates during writing	Periodical drift measurement, precompensation of drift prediction
Error of circular shape of zones due to spindle runout	Real-time correction of reproducible spindle trajectory
Errors of absolute radial coordinate of writing spot	System calibration, correction
Angular coordinate error	System calibration, correction

Generalized error budget of the CLWS system for CGH fabrication

As shown in the previous section, the CLWS demonstrates patterning accuracies sufficient for creating diffraction limited wavefronts. To predict the wavefront irregularities for CGH structures in general, the error contributions of the individual effects need to be evaluated. Therefore, two patterning error contributions of the CLWS are monitored regularly: Figure 5a shows the induced wavefront error as a function of the measured positioning error for one of the fabricated CGHs with 146 mm diameter, having an rms error of 0.006 λ, corresponding to 4 nm. Figure 5b shows the trajectory of rotation of the spindle or spindle run out of the air beared CLWS spindle. This effect leads to an rms wavefront error of 0.004 λ (or 2.5 nm)

Table 3 shows the total error budget of the CGH, including substrate effects. The total error of the wavefront of the produced CGH is 0.013 λ (or 8 nm), with the dominant contribution being the flatness of the substrate itself.

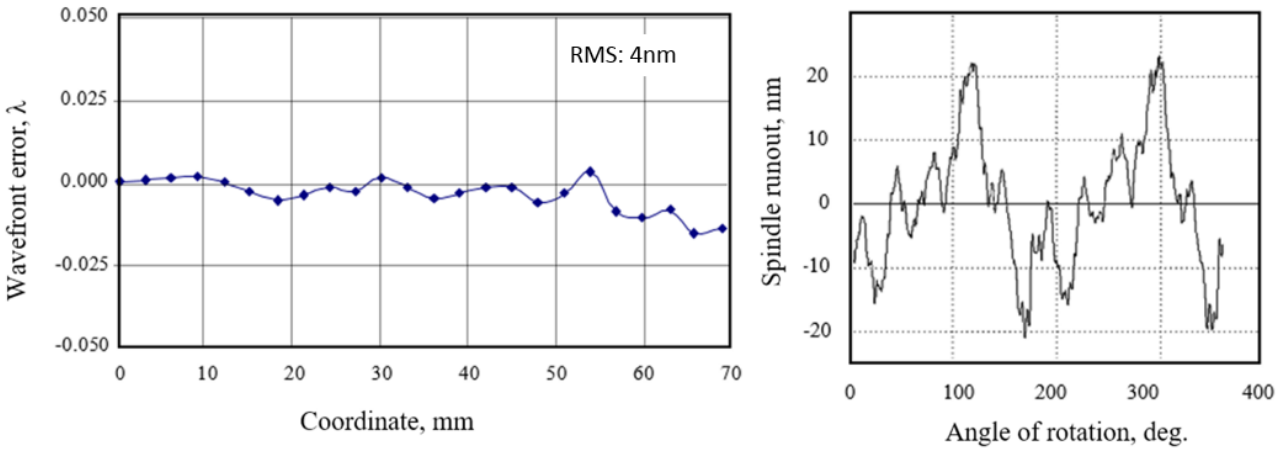

Figure 5. Measured positioning error during CGH writing (a) and CLWS spindle runout (b).

Table 3. Error budget of the CGH

Error contribution	rms value / λ
Flatness of the substrate	0,011
Wavefront errors caused by drift	0,006
Wavefront errors caused by spindle rotation trajectories	0,004
Total error (RSS):	0,013

4. EXPERIMENTAL VERIFICATION OF THE CLWS PATTERNING ACCURACY USING A FZP TYPE CGH

The most common application for the CGHs fabricated on the CLWS is the interferometric test of aspheres. In this case, the CGH generates an aspherical wavefront, which is designed in a way, that it hits the nominal shape of the surface under test in a perfectly perpendicular incidence, thus realizing a so-called Null test. One relies on the diffracted aspherical wavefront as a 'golden standard' and uses the test results for iteratively optimizing the asphere shape. But there is always the possibility that the Null CGH might be defectively produced so that the resulting asphere could be incorrect.

For spherical CGHs or Fresnel zone plates (FZPs), the verification of the wavefront accuracy can be done using a calibrated reference sphere, thus giving an upper estimate of the CGH error. One can also create a CGH which in the ideal case reflects an incident spherical wavefront, thus imitating a reflective sphere. Such a diffractive imitator CGH (DI) can also be used to verify refractive Null tests for aspheres [20].

For the experimental verification of the CGH writing process, a DI of a reflecting spherical mirror with a diameter of 200 mm and a radius of curvature of R = 600 mm, leading to minimum periods of the circular chromium zones of d_min = 1.9 µm was fabricated on an optical substrate with a flatness of 0.01 λ (rms) and a diameter of 230 mm [21,22]. An analysis of the diffracted reflected wavefront of the DI was carried out with a Fizeau interferometer, using a transmission sphere lens TS with f-number f/2.4. The TS forms a spherical wavefront W_s which is diffracted and reflected from the DI back into the interferometer. Figure 6 shows the optical layout of the test and the resulting interferogram with wavefront map. The irregularity of the wavefront was measured to W_{DI} = 0.059 λ (P-V) and 0.0092 λ (rms). This wavefront error corresponds to a patterning error of 20 nm. This value is an upper estimate, because it also includes both the surface figure error of the optical substrate of the DI and of the TS.

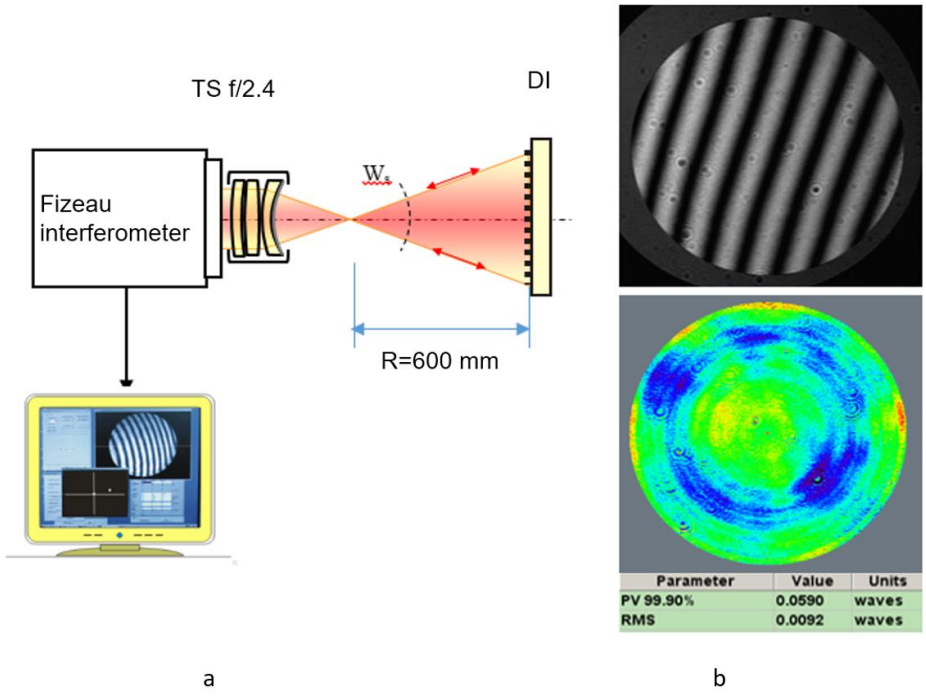

Figure 6 .Optical layout for testing a diffractive imitator CGH (a), resulting phase map of the reflected wavefront (b).

5. EXPERIMENTAL VERIFICATION OF THE MZ-CGH

The previous section describes a verification of the CLWS accuracy in terms of the quality of a generated wavefront. As pointed out in section 2, the key feature of MZ-CGHs for alignment purposes is however the straight line (optical axis) defined by the series of foci from the different zones. The straightness as well as the correct distance between the spots are accordingly essential prerequisites for the success of the method and therefore explicitly verified.

A sketch of the experimental setup is shown in Figure 7. A high precision air bearing translation stage, built up of hard stone (granite) with an aluminium carriage, is aligned parallel to the optical axis of the MZ-CGH with an accuracy in the sub-micron range. This task is facilitated with the help of a hexapod with definable pivot point. The position of the carriage along the direction of motion is optically detected with a contactless measuring tape with a graduation period of 20 µm and a spatial resolution of 0.1 µm. The linearity is specified as ± 3 µm over a distance of 1 m and 0.75 µm over 60 mm. The measuring tape is bonded to the granite core of the stage and behaves thermally like this substrate (linear expansion coefficient $\alpha \approx 3$ µm/m/K).

We present two different approaches: Detection of the spots with a cooled low noise measurement camera and interferometrical test with a reference sphere replacing the camera.

Spot detection with measurement camera

In the case of the camera measurement, an optical magnification with a micro objective - tube lens combination by a factor of 30.3 yields an effective pixel size of 0.15 µm. The center of mass of each spot can be determined with an accuracy of typically up to about 1/10 of the pixel size, which is only 15 nm. The straightness tolerance of the translation stage is specified with a maximum deviation of 2.5 µm over the whole travelling distance of 800 mm. This remaining error is eliminated by calculating the differences of the spot positions for two measurement sequences, whereas the MZ-CGH is rotated in between by 180°.

The upper plots of Figure 8 shows the so determined lateral spot center of mass positions (blue circles), averaged over 50 camera shots, along the nominal z-position together with a linear fit (red line). The circle diameter is chosen in the order of the standard deviation σ of the 50 frames. The lower plots indicate the residuals between spot position and linear fit. The *norm* of the residuals (defined as the square root of the sum of the squares of the residuals) is printed inside the plots. As result, the observed deviation of the 5 spots from a straight line is < 0.2 µm. This outcome is well reproduced in repeated measurements. Included as error budget are measurement errors due to mechanical and thermal drifts.

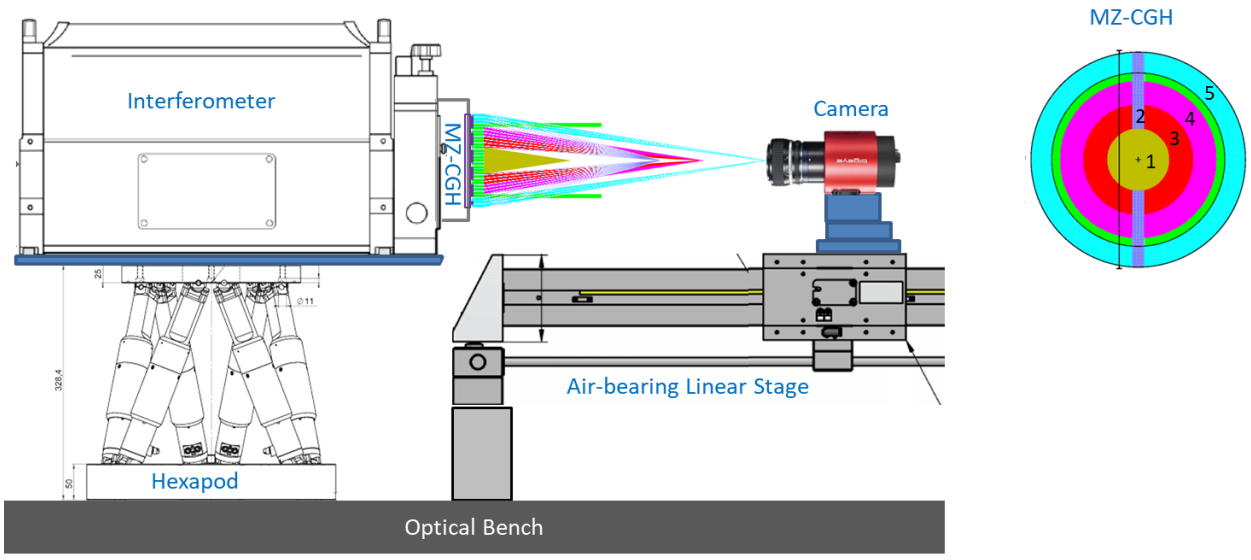

Figure 7. Setup for verifying the straightness of the optical axis of a MZ-CGH.

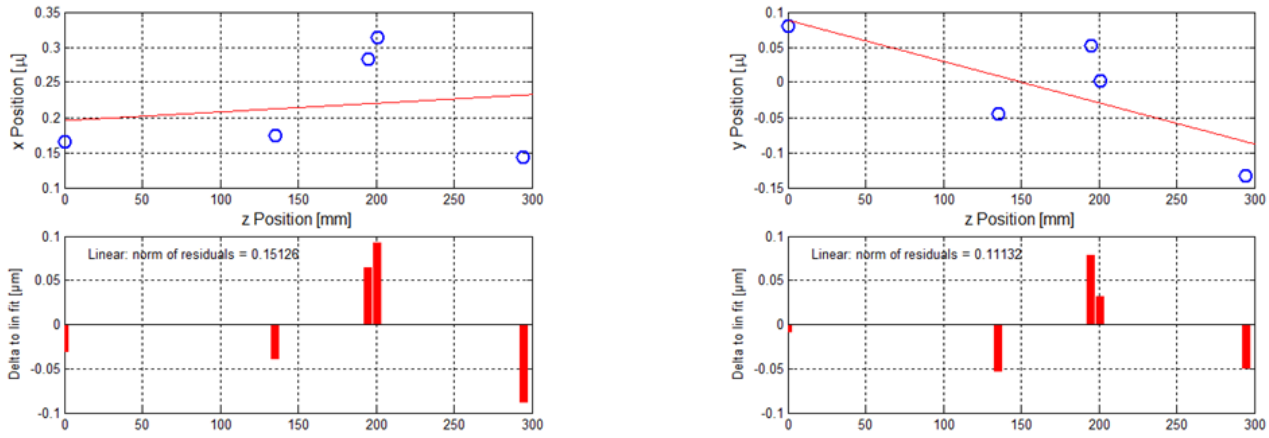

Figure 8. Measurement of the straightness of the focal spot positions of a MZ-CGH. Note the tiny range in the lateral direction!

Interferometrical test with reference sphere

For the second approach, the camera in Figure 7 is replaced by a reflecting reference sphere with high optical surface quality, which is moved along the linear stage. This setup is similar to the later alignment procedure of the lens assembly.

The five spherical wavefront segments with the reference sphere moved to its corresponding nominal autocollimation positions are measured in Figure 9. The P-V error is in the range between 0.1 and 0.2 λ.

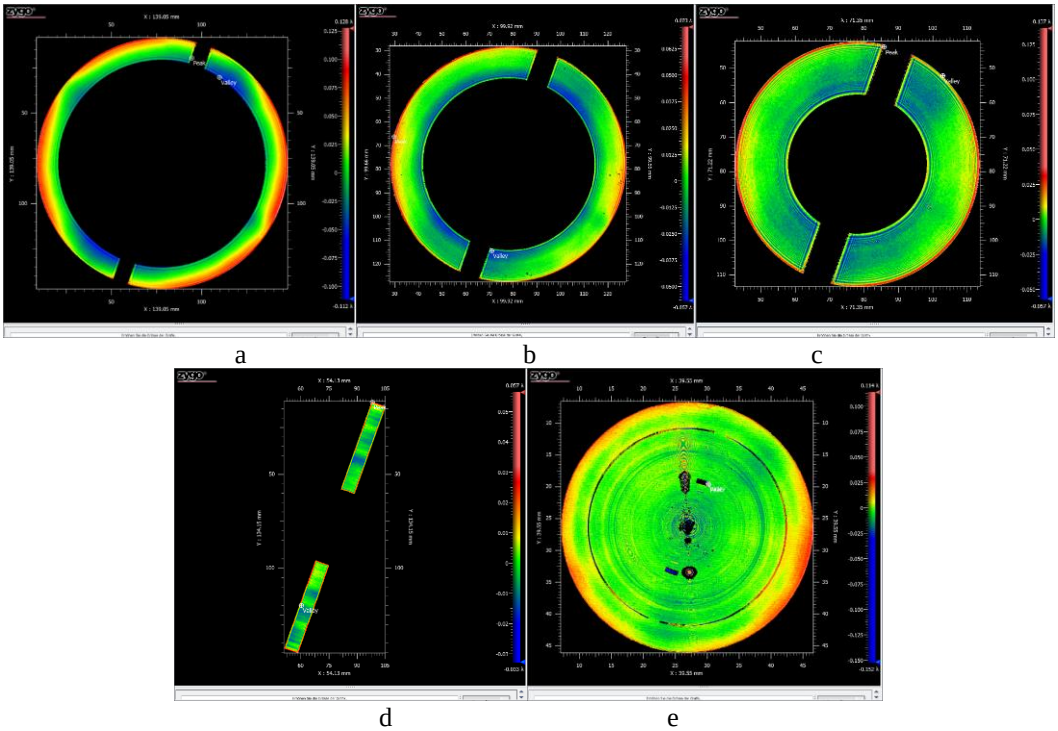

Figure 9. Measurement of the five spherical wavefront segments of the MZ-CGH. L3 (a), L2 (b) and L1 (c). Cat-eye signals: L3 (d), and L1 (e)

As described in section 2, the most important signals for the alignment strategy are however the tip, tilt and defocus (power) Zernike coefficients. As an example, Figure 10 shows the defocus coefficient as function of the distance along the optical axis for the cat-eye spot on L1 around the nominal Null fringe position (blue circles). The linear fit allows a sensitive determination of the position, in this case with an accuracy in the sub µm range. The exact quantitative relations will be analyzed in Ref. [7].

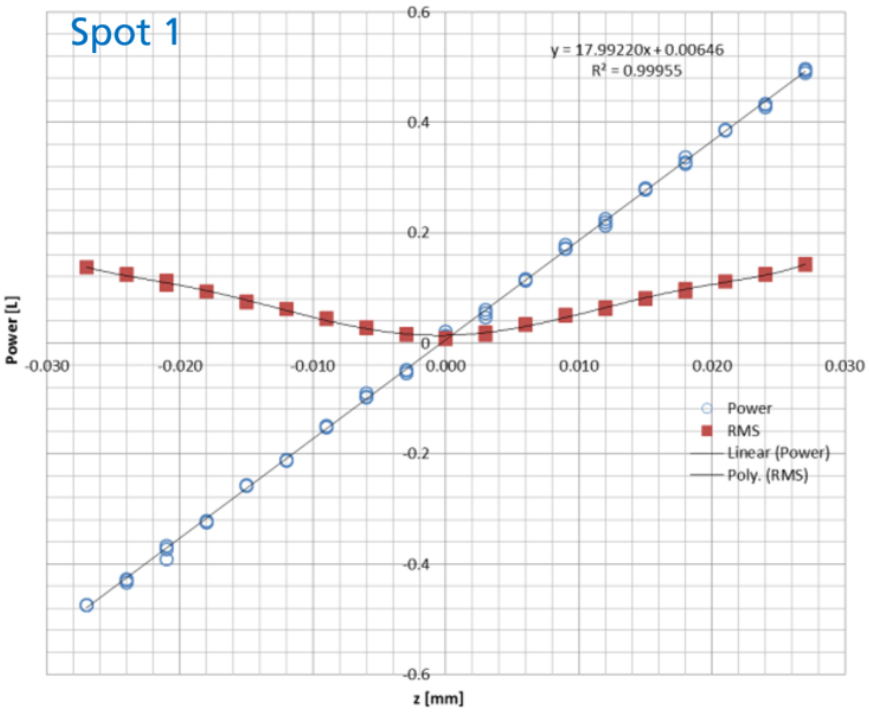

Figure 10. Blue circles: Defocus Zernike coefficient as function of the distance along the optical axis for the cat-eye spot on L1 around the nominal Null fringe position. Red squares: RMS of the wavefront including defocus.

The distance between the five spots of the MZ-CGH can be determined with high accuracy as the difference between the crossings of the linear fits with the defocus (power) axis in Figure 10. As result, 4 spots meet their nominal position within the expected measurement accuracy of about 2.5 µm. The spot from the outermost annular zone (cyan rays, labeled with number 5 in Figure 7) with the largest focal length (f = 379.395 mm) turns out to be reproducibly (6 ± 2.5) µm too close. A detailed analysis follows in a recent publication.

6. CONCLUSION

A multi-zone CGH was fabricated on the high precision circular laser writing system (CLWS). For this purpose, a resistless laser direct writing method onto a chromium film with subsequent reactive ion beam etching was used. The wavefront precision of the manufactured CGH consisting of a set of different Fresnel Zone Plate areas was verified using a reference sphere and a Fizeau interferometer and yielded a surface figure error of < 0.2 λ P-V.

The straightness as well as the correct distance between the series of spots generated by the multi-zone CGH are essential prerequisites for the success of the demonstrated alignment procedure and therefore explicitly verified. As result, the observed deviation of the 5 spots from a straight line is < 0.2 µm. This outcome is well reproduced in repeated measurements. Included are measurement errors due to mechanical and thermal drifts.

The distance between the five spots of the MZ-CGH along the optical axis yielded the following findings: Four spots meet their nominal position within the expected measurement accuracy of about 2.5 µm. The spot from the outermost annular zone with the largest focal length (f = 379.395 mm) turns out to be reproducibly (6 ± 2.5) µm too close. Measurement errors are expected mainly due to the accuracy of the measuring tape as well as mechanical and thermal drifts.

A detailed analysis follows in a recent publication.

7. ACKNOWLEDGEMENTS

This work was done in close cooperation between the Max Planck Institute for Extraterrestrial Physics and Dioptic and under a scientific cooperation agreement between IA&E SB RAS and Dioptic GmbH. The development of the CGH fabrications and tests are supported by the Russian Science Foundation under grant No 17-19-01721. The MPE Euclid participation is supported by DLR under grant 50 QE 1101.

8. REFERENCES

[1] Laureijs, R. J. e. a., “Euclid definition study report (Red Book)”, ESA/SRE(2011)12 1 (2011).

[2] http://sci.esa.int/euclid/; http://www.euclid-ec.org/.

[3] Grupp, F.; Prieto, E.; Geis, N.; Bode, A.; Bodendorf, C.; Costille, A.; Katterloher, R.; Penka, D.; Bender, R., “Final tolerancing approach and the value of short-cutting tolerances by measurement”, Proc. SPIE 9904, Space Telescopes and Instrumentation 2016: Optical, Infrared, and Millimeter Wave, 99042M (29 July 2016).

[4] Frank Grupp, Eric Prieto, Norbert Geis, Andreas Bode, Reinhard Katterloher, Christof Bodendorf, Daniela Penka, and Ralf Bender, “The EUCLID NISP tolerancing concept and results”, Proc. SPIE 9143, 91432X (2014).

[5] Chr. Bodendorf; A. Bode; N. Geis; D. Penka; F. Grupp; R. Bender „Performance measurement of high precision optical assemblies for cosmological observations: comparison of different approaches”. Proc. SPIE 10009, Third European Seminar on Precision Optics Manufacturing, 100090F (June 30, 2016).

[6] C. Gal et al. “Development and verification of high precision cryogenic lens holders”, ICSO 2014.

[7] Chr. Bodendorf et al. “Computer generated holograms for high-precision optical adjustment purposes. Part I: Analytical sensitivity analysis” to be published.

[8] A.G. Poleshchuk, E.G. Churin, V.P. Koronkevich, V.P. Korolkov. "Polar coordinate laser pattern generator for fabrication of diffractive optical elements with arbitrary structure", Applied Optics, 38, 1295-1301 (1999).

[9] A.G. Poleshchuk, V.P. Koronkevich, V.P. Korolkov, A.A. Kharissov, V.V. Cherkashin, "Fabrication of diffractive optical elements in the polar coordinate system: fabrication errors and their measurement", Optoelectronics Instrumentation and Data Processing, N 6, 40-53 (1997).

[10] Y.V. Chugui, A.G. Verkhoglyad, P.S. Zavyalov, E.V. Sysoev, R.V. Kulikov, I.A. Vykhristyuk, M.A. Zavyalova, A.G. Poleshchuk, V.P. Korolkov. “Optical Measuring and Laser Technologies for Scientific and Industrial Applications”, Int. J. of Automation Technology, 9, No.5, p. 515–524. (2015).

[11] A. G. Poleshchuk; V. P. Korolkov and R.K. Nasyrov, "Diffractive optical elements: fabrication and application ," Proc. SPIE 9283, 928302 (2014).

[12] V.V. Cherkashin, E. G. Churin, V. P. Korolkov, V.P. Kooronkevich, A.A. Kharissov, A.G. Poleshchuk, J.H. Burge, “Processing parameters optimisation for thermochemical writing of DOEs on chromium films”, Proc. SPIE. 3010, 168-179 (1997).

[13] V.V. Cherkashin, A.A. Kharissov, V.P. Korolkov, V. P. Koronkevich, A. G. Poleshchuk, “Accuracy potential of circular laser writing of DOEs”, Proc. SPIE 3348, 58-68 (1998).

[14] A.G. Poleshchuk, V.P. Korolkov, V.V. Cherkashin, S. Reichelt, J.H. Burge. “Methods for minimizing the errors in direct laser writing of diffractive optical elements”, Optoelectronics, Instrumentation and Data Processing, 38, No. 3, 3-13 (2002).

[15] V.V. Cherkashin, E.G. Churin, V.P. Korolkov, et al., “Processing Parameter Optimization for Thermochemical Writing of DOEs on Chromium Films”, Proc. SPIE 3010, 168–179 (1997).

[16] A.G. Poleshchuk, V.P. Koronkevich, V.P. Korolkov, et al., “Synthesis of Diffractive Optical Elements in a Polar Coordinate System: Fabrication Errors and their Measurement”, Optoelectronics, Instrumentation and Data Processing, No. 6, 42–56 (1997).

[17] Yu-Chun Chang and J.H. Burge, “Error analysis for CGH optical testing,” Proc. SPIE 3782, 358-366 (1999).

[18] A.G. Poleshchuk, V.P. Korolkov, V.V. Cherkashin, J. Burge.”Methods for certification of CGH fabrication,” Trends in Optics and Photonics, (OSA Topical Meeting "DOMO-2002", June 3-6, 2002, Tucson, USA). 75, 438-440 (2002).

[19] R.K. Nasyrov, A.G. Poleshchuk, V.P. Korolkov, K. Pruss, S. Reichelt. “Certification of diffractive optical elements for aspherical optics testing”, Optoelectronics, Instrumentation and Data Processing. 41 No. 1, 100-108 (2005).

[20] N.P. Larionov, A.V. Lukin, R.A. Rafikov. “Imitator of main telescope mirror on the base of CGH”, Journal of Optical Technology, No 1, 39-40 (1980).

[21] R.V. Shimanskii, A.G. Poleshchuk, V.P. Korolkov, and V.V. Cherkashin, “Dynamic correction of the laser beam coordinate at fabrication of large-sized diffraction elements for the testing of aspherical mirrors”, Optoelectronics, Instrumentation and Data Processing. 53, No. 3, pp. 64–73 (2017).

[22] R.V. Shimanskii, A.G. Poleshchuk, V.P. Korolkov, and V.V. Cherkashin. “Alignment of the Writing Beam with the Diffractive Structure Rotation Axis in Synthesis of Diffractive Optical Elements in a Polar Coordinate System”, Optoelectronics, Instrumentation and Data Processing. 53, No. 2, pp. 123-131 (2017).